



EUROfusion

WPPFC-CPR(18) 18763

H Maier et al.

Deuterium retention in tungsten-based materials for fusion applications

Preprint of Paper to be submitted for publication in Proceeding of 23rd International Conference on Plasma Surface Interactions in Controlled Fusion Devices (PSI-23)



This work has been carried out within the framework of the EUROfusion Consortium and has received funding from the Euratom research and training programme 2014-2018 under grant agreement No 633053. The views and opinions expressed herein do not necessarily reflect those of the European Commission.

This document is intended for publication in the open literature. It is made available on the clear understanding that it may not be further circulated and extracts or references may not be published prior to publication of the original when applicable, or without the consent of the Publications Officer, EUROfusion Programme Management Unit, Culham Science Centre, Abingdon, Oxon, OX14 3DB, UK or e-mail Publications.Officer@euro-fusion.org

Enquiries about Copyright and reproduction should be addressed to the Publications Officer, EUROfusion Programme Management Unit, Culham Science Centre, Abingdon, Oxon, OX14 3DB, UK or e-mail Publications.Officer@euro-fusion.org

The contents of this preprint and all other EUROfusion Preprints, Reports and Conference Papers are available to view online free at <http://www.euro-fusionscipub.org>. This site has full search facilities and e-mail alert options. In the JET specific papers the diagrams contained within the PDFs on this site are hyperlinked

Deuterium retention in tungsten based materials for fusion applications

H. Maier^{a*}, T. Schwarz Selinger^a, R. Neu^{a,b}, C. Garcia-Rosales^{c,d}, M. Balden^a, A. Calvo^{c,d}, T. Dürbeck^a, A. Manhard^a, N. Ordás^{c,d}, T. F. Silva^{a,e}

^aMax-Planck-Institut für Plasmaphysik, Boltzmannstr. 2, 85748 Garching, Germany

^bTechnische Universität München, Boltzmannstrasse 15, 85748 Garching, Germany

^cCeit-IK4, Paseo de Manuel Lardizabal 15, 20018 San Sebastian, Spain

^dUniversidad de Navarra, Tecnun, Paseo de Manuel Lardizabal 13, 20018 San Sebastian, Spain

^eInstituto de Física da Universidade de São Paulo, Rua do Matão, trav. R 187, 05508-090 São Paulo, Brazil

*Corresponding author:

Hans Maier

Max-Planck-Institut für Plasmaphysik

Boltzmannstr. 2

85748 Garching

Germany

Email: Hans.Maier@ipp.mpg.de

phone: +49 89 3299 1805

Highlights:

- tungsten alloys were investigated for their deuterium retention
- The “heavy alloy” HPM 1850 retains similar amounts as pure tungsten
- The self-passivating alloy W10Cr0.5Y retains 10 times more

1 Deuterium retention in tungsten based materials for fusion applications

2 H. Maier^{a*}, T. Schwarz-Selinger^a, R. Neu^{a,b}, C. Garcia-Rosales^{c,d}, M. Balden^a, A. Calvo^{c,d}, T.
3 Dürbeck^a, A. Manhard^a, N. Ordás^{c,d}, T. F. Silva^{a,e}

4 ^aMax-Planck-Institut für Plasmaphysik, Boltzmannstrasse 2, 85748 Garching, Germany

5 ^bTechnische Universität München, Boltzmannstrasse 15, 85748 Garching, Germany

6 ^cCeit-IK4, Paseo de Manuel Lardizabal 15, 20018 San Sebastian, Spain

7 ^dUniversidad de Navarra, Tecnum, Paseo de Manuel Lardizabal 13, 20018 San Sebastian,
8 Spain

9 ^eInstituto de Física da Universidade de São Paulo, Rua do Matão, trav. R 187, 05508-090 São
10 Paulo, Brazil

11 12 Abstract

13 The tungsten “heavy alloy” HPM 1850, a liquid-phase sintered composite material with two
14 weight percent Ni and one weight percent Fe as well as the self-passivating tungsten alloy W-
15 10Cr-0.5Y, a high temperature oxidation resistant alloy with 10 weight percent of Cr and 0.5
16 weight percent of Y were investigated with respect to their deuterium retention. The samples
17 were deuterium loaded in an electron cyclotron resonance plasma up to a fluence of 10^{25}m^{-2} .
18 The deuterium retention was then investigated by Nuclear Reaction Analysis and by Thermal
19 Desorption. In HPM 1850 the observed deuterium amount was similar to pure tungsten,
20 however the outgassing behaviour during thermal desorption was considerably faster. In W-
21 10Cr-0.5Y the released deuterium amount during thermal desorption was about one order of
22 magnitude higher; by comparison of nuclear reaction analysis and thermal desorption this was
23 attributed to faster diffusion of deuterium into the bulk of the material.

24 Keywords: deuterium retention, tungsten heavy alloy, tungsten self-passivating alloy, nuclear
25 reaction analysis, thermal desorption

26 27 28 1 Introduction

29 The general present-day assumption for the choice of plasma-facing materials in future fusion
30 devices is to use tungsten for both, the divertor and the main chamber wall, see for instance
31 [1]. These applications, however, pose very different requirements to the materials properties.
32 While a divertor target material must have sufficient toughness to withstand high thermo-
33 mechanical loads, a main chamber plasma-facing material must protect the underlying steel
34 structures from erosion without bearing high thermo-mechanical loads. The tritium retention
35 in the near-surface region of the plasma-facing material, the re-emission, and the diffusion of
36 tritium into the bulk are of importance for the tritium inventory in future fusion devices [2].

37 This is especially important for main chamber materials because of the large surface area of
38 the main chamber first wall in a fusion reactor.

39 In the European fusion community a long-term materials development programme has been
40 conducted in the frame of the EUROfusion Workpackage Materials, which also included the
41 development of several tungsten-based materials for divertor as well as main chamber wall
42 application [3, 4]. With respect to the plasma-material interaction properties the fusion
43 community can readily refer to well-reviewed data for pure tungsten [5, 6]. There are,
44 however, no data available for tungsten-based materials, which are new in the fusion
45 community. The purpose of this contribution is to present first data for two tungsten-based
46 materials with respect to their deuterium retention and to compare this with a reference
47 tungsten material. For this purpose deuterium was implanted from an electron cyclotron
48 resonance plasma and the retention was analysed by Nuclear Reaction Analysis (NRA) and
49 Thermal Desorption (TD). This activity was performed in the frame of the EUROfusion
50 Workpackage Plasma-Facing Components (PFC), see for instance [7].

51 The materials under investigation here are a so-called tungsten heavy alloy, which could be
52 employed as an alternative divertor target material [8], and a self-passivating tungsten alloy
53 [9], an oxidation-resistant material, which was developed in the frame of the EUROfusion
54 Workpackage Materials to be employed on the main chamber wall of a fusion reactor. These
55 materials will be described in more detail in section 2. Section 3 gives the experimental
56 details and procedures. The experimental results and a discussion are presented in section 4.

57 **2 The Materials**

58 **2.1 Tungsten Heavy Alloy**

59

60 The so-called tungsten heavy alloy is a two-phase composite material consisting of tungsten
61 powder particles in a matrix of a metal with lower melting point. It is produced by liquid
62 phase sintering. In the original publication either copper or nickel were proposed as matrix
63 material [10]. Here we investigate a commercially available material of tungsten with two
64 weight percent nickel and one weight percent iron. The density of this material is 18.5 g/cm^3 ;
65 it was purchased from HC Starck Hermsdorf GmbH, Germany and is labelled HPM 1850.

66 After a thorough pre-characterisation including high heat flux testing, which was reported in
67 [11], this material was employed as a divertor target material in the tokamak ASDEX
68 Upgrade. Because of its better mechanical properties the use of HPM 1850 was proposed to
69 eliminate problems with cracking of bulk tungsten tiles, which were reported in [12]. The
70 positive results of this measure are reported in detail in [8].

71 Figure 1 shows the microstructure of HPM 1850: It consists of tungsten powder grains of
72 sizes of a few $10 \text{ }\mu\text{m}$ up to more than $100 \text{ }\mu\text{m}$ surrounded by the nickel/iron matrix.

73

74

75 **2.2 Self-Passivating Tungsten Alloy**

76

77 In the case of a loss of coolant the plasma-facing surfaces of a fusion reactor can reach high
78 temperatures due to residual decay heat. In the European Power Plant Conceptual Studies
79 PPCS it was shown that the outboard first wall of the reactor concepts A, B, and C can reach
80 temperatures in excess of 1000°C within days or tens of days [13]. In such a situation the
81 ingress of oxygen would lead to the formation of volatile and radioactive WO_3 , see [14] and
82 references therein. For this reason it was proposed in [14] to use self-passivating alloys as
83 plasma-facing materials on the first wall. In such an alloy the alloying elements form a stable
84 oxide layer on the surface when exposed to oxygen which prevents further oxidation of the
85 material. The composition we investigate in this contribution consists of tungsten with 10
86 weight percent of chromium and 0.5 weight percent of yttrium as alloying elements, labelled
87 W-10Cr-0.5Y. It is produced at CEIT, San Sebastian by mechanical alloying and hot isostatic
88 pressing. Its density is 99.7% of the theoretical value from the rule of mixture. An SEM image
89 of this material is shown in figure 2. The material consists of a tungsten-rich phase, which
90 appears in light grey and a chromium-rich phase in black. The typical grain size is on the
91 order of 100 nm. Further details can be found in [9].

92

93 **2.3 Tungsten Reference Material**

94

95 The tungsten reference material was exposed to the deuterium plasma in parallel with the
96 respective self-passivating alloy and heavy alloy samples for comparison.

97 It is a hot-rolled polycrystalline tungsten material from Plansee SE with a specified purity of
98 99.7 %. The typical grain size is in the micrometre range, as shown in figure 3. A detailed
99 microstructural analysis of this material including the effect of an annealing step at 930°C can
100 be found in [15].

101 **3 Experimental Procedures**

102

103 Samples of W-10Cr-0.5Y, HPM 1850, and tungsten reference material were polished and pre-
104 characterised by microscopy. After outgassing them in vacuum at 930°C the samples were
105 loaded with deuterium in an ECR plasma device. Then the deuterium retention was analysed
106 by Nuclear Reaction Analysis (NRA) and subsequently Thermal Desorption (TD) was
107 performed. In the following the procedures for deuterium loading as well as NRA and TD
108 analysis are given in more detail.

109 **3.1 Deuterium Loading**

110

111 Deuterium loading of the samples was performed by exposing them to a deuterium plasma
112 from an ECR plasma source described in [16]. The plasma ions from this source are mostly

113 D_3^+ ions. Only 3 % of the impinging D flux arrives at the samples in the form of D^+ and D_2^+
114 ions.

115 D loading was performed at a sample temperature of 100°C and a bias voltage corresponding
116 to 38 eV/D for the D_3^+ ions. Three sets of samples were exposed to D fluences of $10^{23}m^{-2}$,
117 $10^{24}m^{-2}$, and $10^{25}m^{-2}$, respectively. At a flux of $10^{20}m^{-2}s^{-1}$ this corresponded to exposure times
118 of 0.3h, 3h, and 30h. With each set one sample of tungsten reference material was also
119 exposed.

120 **3.2 Nuclear Reaction Analysis**

121

122 Nuclear Reaction Analysis was performed using the 3 MeV tandem accelerator at the Max-
123 Planck-Institut für Plasmaphysik in Garching.

124 Using the $D(^3He,p)\alpha$ reaction at 3He beam energies up to 6.0 MeV and detecting the high
125 energy protons allows probing the D content in the W samples up to a depth of approximately
126 10 μm . Using the software NRADC to deconvolute the proton spectra from different 3He
127 beam energies, concentration depth profiles can be constructed. In our analysis we used 6
128 different energies between 0.69 MeV and 6.0 MeV. NRADC is described in detail in
129 reference [17]. It is based on a Markov chain Monte Carlo approach and is especially
130 designed and optimised for the construction of trace element depth profiles. The software uses
131 the SIMNRA program [18] to compute proton spectra. A subset of our data was also analysed
132 using the independent computer code MULTISIMNRA [19]. MULTISIMNRA is a general
133 purpose tool for analysing sets of ion beam spectra by running multiple instances of SIMNRA
134 and performing multi-dimensional fits. The deuterium concentration depth profiles produced
135 by using NRADC and MULTISIMNRA coincide within the error ranges given by the
136 respective software package.

137 **3.3 Thermal Desorption**

138

139 Thermal desorption was performed in the setup described in reference [20]. Basically it
140 consists of a stainless steel vacuum vessel with a quadrupole mass spectrometer at a base
141 pressure in the 10^{-10} mbar range. Via a metal glass transition a quartz glass tube is attached to
142 the vessel, which contains the samples at a base pressure in the 10^{-8} mbar range. The samples
143 can be heated up to 1050°C by moving a tubular furnace over the quartz glass tube. In our
144 experiments a heating ramp of 15 K/min was used.

145 For the pure tungsten reference samples the temperature was ramped up to 1050°C. For the
146 alloys the heating ramps were stopped at 850°C. This was done because of the higher vapour
147 pressures of the alloying metals as compared to that of pure tungsten.

148 The mass-4 signal of the mass spectrometer when detecting D_2 gas is calibrated by injecting a
149 calibrated flux of deuterium gas into the vessel. For deuterium arriving at the mass
150 spectrometer in the form of HD molecules a calibration using a calibrated volume and a
151 spinning rotor pressure gauge was used as explained in reference [21]. A part of the released

152 deuterium, however, arrives at the mass spectrometer in the form of water HDO or D₂O,
153 respectively, i.e. at the masses 19 and 20. For these a direct calibration factor is not available.
154 In our measurements the relative amount of deuterium released in the form of water decreases
155 substantially with increasing implantation fluence. Assuming the same sensitivity of the setup
156 for HDO and D₂O as for the HD signal from mass 3, we estimate it to range from about 20-
157 35% at the lowest applied implantation fluence to 4-7% at the highest fluence.

158 **4 Results and Discussion**

160 **4.1 HPM 1850**

162 Figure 4 shows the integrated amounts of deuterium released during the thermal desorption
163 ramp as a function of implantation fluence for two HPM 1850 samples at each fluence in
164 comparison with the reference tungsten material. In these datasets the mass spectrometer
165 signals for all masses discussed in section 3c are included, i.e. D₂, HD, HDO, and D₂O. As the
166 figure shows, the total released amount is the same for HPM 1850 and the reference tungsten
167 within a factor of 2. The fact that the trend is reversed from the lowest to the highest
168 implantation fluence can possibly be related to the uncertain contribution of the masses 19
169 and 20, as discussed in section 3c.

170 Figure 5 shows thermal desorption data from two HPM 1850 samples implanted with a
171 deuterium fluence of 10²⁵m⁻² in comparison with a reference tungsten sample implanted with
172 the same fluence. The temperature ramp is 15 K/min. For the pure tungsten sample the
173 temperature was ramped up to 1050°C while for the alloy it was limited to 850°C. As the
174 figure shows, for both HPM 1850 samples the deuterium release occurred at lower
175 temperatures than for the tungsten reference sample. This indicates either a faster out-
176 diffusion or lower trap binding energies in the HPM 1850 material as compared to the
177 reference tungsten material.

178 In reference [22] hydrogen diffusion coefficients for the pure metals nickel and iron are given.
179 According to this reference the activation energy for hydrogen diffusion in nickel is very
180 similar to the tungsten case, i. e. about 0.4 eV, while in iron the activation energy is
181 significantly lower. Reference [23] shows in detail that the activation energy for hydrogen
182 diffusion in Ni/Fe alloys actually is a function of the alloy composition and depends on the
183 thermal history of the sample. Depending on the heat treatment, which was also performed in
184 our case, the activation energy for hydrogen diffusion in Ni/Fe alloys can have a minimum of
185 less than 0.2 eV in the compositional range of 70% to 80% Ni. As this is close to the
186 composition of the matrix material in HPM 1850, this could be the reason why the out-
187 diffusion occurs considerably faster during the temperature ramp in the desorption
188 experiment. However, this would only hold for hydrogen atoms diffusing in the Ni/Fe matrix.
189 Reference [24] gives enthalpies of solution for hydrogen in pure nickel or pure iron which are
190 considerably lower than that of tungsten. Data on the enthalpy of solution of deuterium in a
191 Ni/Fe alloy with the actual composition of our sample material are not available. However, if

192 we assume the trend given for the pure materials to hold also for the alloy, then this would
193 additionally support the faster out-diffusion process, because hydrogen atoms would
194 energetically prefer the Ni/Fe matrix from the tungsten grains. In summary this would mean
195 that hydrogen atoms entering the matrix material would stay in there and leave the sample in a
196 faster diffusion process compared to tungsten.

197

198

199 **4.2 W-10Cr-0.5Y**

200

201 Figure 6 shows the total released amounts of deuterium from the W-10Cr-0.5Y samples in
202 comparison with the reference tungsten material. Here we have 2 data points for the highest
203 and lowest deuterium implantation fluence at 10^{23}m^{-2} and 10^{25}m^{-2} , and only one data point at
204 the intermediate fluence of 10^{24}m^{-2} . The data for the tungsten reference material are the same
205 as in figure 4 and are plotted here for comparison.

206 The figure clearly shows that the amount of deuterium released by the W-10Cr-0.5Y alloy is
207 roughly an order of magnitude higher than the corresponding amount from the tungsten
208 reference material. This observation holds for the whole investigated implantation fluence
209 range, which spans 2 orders of magnitude, and shows to be well reproducible in the cases
210 where two samples per fluence were employed.

211 In figure 7 a comparison of the TD data from figure 6 with the corresponding NRA data from
212 the same samples is shown: As in figure 6 the TD data from the W-10Cr-0.5Y samples are
213 represented by the blue crosses and green squares and the TD data from the tungsten reference
214 samples are represented by closed black squares. For all samples the NRA data were obtained
215 several days before outgassing the samples in the TD setup. They are shown as blue and green
216 open circles and as black open squares, respectively, for the two sample types. The
217 comparison shows that with increasing implantation fluence the integrals of the TD data
218 increase systematically, while the integrated NRA data stay approximately constant for the
219 two higher fluences of 10^{24}m^{-2} and 10^{25}m^{-2} . At the highest fluence there is a discrepancy of
220 about one order of magnitude. In contrast to this, for the tungsten reference material the TD
221 data and the NRA data for the two higher fluences coincide approximately.

222 In our interpretation this comparison shows that with increasing fluence, which corresponds to
223 increasing implantation time, in the case of W-10Cr0.5-Y the implanted deuterium diffuses
224 deeper into the material, such that at the two longer implantation times in our experiment
225 most of the deuterium already diffused beyond the information depth of our NRA depth
226 profiling measurements, which is about $10\ \mu\text{m}$. Therefore the TD analysis shows a larger
227 amount of deuterium, which cannot be detected by the NRA measurements, since it is mostly
228 trapped beyond the NRA information depth.

229 A similar observation was made in a different tungsten alloy: In reference [25] it was
230 observed that alloying of tungsten with 1% or 5% of tantalum, respectively, led to an increase
231 of the retained amount of deuterium by roughly one order of magnitude for implantation

232 fluences in the range of 10^{24}m^{-2} , which is similar to the fluence range investigated here. In the
233 data shown in [25], however, there is a clear fluence dependent increase of the relative
234 deuterium retention with increasing implantation fluence, which does not show in our data.
235 Different from our interpretation presented here, the authors of [25] conclude from a
236 comparison of their results with modelling, that the increased retention is due to an increase of
237 the trap density in the material caused by tantalum alloying rather than due to deeper
238 diffusion.

239 **5 Summary, Conclusions, and Outlook**

240

241 We performed an investigation of the deuterium retention in two materials, which are new in
242 the fusion community: the tungsten heavy alloy HPM 1850, which is a liquid phase sintered
243 material of tungsten with 3 weight percent of nickel and iron and a self-passivating alloy of
244 tungsten with 10 weight percent of chromium and 0.5 weight percent of yttrium, W-10Cr-
245 0.5Y, which is a material resistant to high temperature oxidation.

246 Samples were loaded with deuterium from an ECR plasma with fluences of 10^{23}m^{-2} , 10^{24}m^{-2} ,
247 and 10^{25}m^{-2} , respectively. These samples were then analysed with Nuclear Reaction Analysis
248 with a ^3He beam of energies in between 0.69 MeV and 6.0 MeV, which allows deuterium
249 depth profiling up to a depth of about 10 μm . Subsequently the samples were outgassed in a
250 Thermal Desorption setup. These results were compared to results from a pure tungsten
251 reference material.

252 It was found that the amount of deuterium released from HPM 1850 samples is very similar to
253 that from pure tungsten, whereas the outgassing occurs faster during the thermal desorption
254 temperature ramp. This was interpreted in terms of faster out-diffusion of deuterium through
255 the Ni/Fe matrix transport channel.

256 For the W-10Cr-0.5Y material it was found that the amount of deuterium released during the
257 thermal desorption temperature ramp is about one order of magnitude higher than the
258 corresponding amount from our reference tungsten material. This is valid for all investigated
259 implantation fluences. By comparing this result with the corresponding result from Nuclear
260 Reaction Analysis depth profiling it was concluded that this observation is due to faster
261 diffusion of deuterium beyond the information depth of the ion beam analysis into the bulk of
262 the samples.

263 For both of the sample materials investigated in this contribution our interpretation of the
264 different behaviour when compared to our reference tungsten material involves diffusion.
265 Therefore the next step will be the investigation of the temperature dependence of the
266 deuterium retention. This will shed more light onto the question whether the diffusion
267 coefficients in the W-10Cr-0.5Y alloy in one case and in the Ni/Fe matrix of HPM 1850 in the
268 other are responsible for the observed differences.

269 The final step of this work will be the investigation of deuterium retention in samples
270 irradiated with high energy ions. This allows the simulation of neutron induced radiation

271 damage by using an MeV accelerator. In the process of the European fusion roadmap the
272 European materials assessment group called the lack of data on the effect of irradiation on the
273 tritium retention of tungsten materials a “highest impact project level risk” for DEMO [26].

274 **Acknowledgement**

275 This work has been carried out within the framework of the EUROfusion Consortium under
276 EUROfusion WP PFC and has received funding from the Euratom research and training
277 programme 2014-2018 under grant agreement No 633053. The views and opinions expressed
278 herein do not necessarily reflect those of the European Commission.

-
- 1 C. Bachmann et al., *Fus. Eng. Des.* 112 (2016) 527
 - 2 Y. Fukai, *The Metal-Hydrogen System*, 2nd edition, Springer, Berlin 2005, chapter 5
 - 3 M. Rieth et al., *J. Nucl. Mater.* 417 (2011) 463
 - 4 M. Rieth et al., *J. Nucl. Mater.* 432 (2013) 482
 - 5 R. Causey, *J. Nucl. Mater.* 300 (2002) 91
 - 6 Ch. Skinner et al., *Fus. Sci. Technol.* 54 (2008) 891
 - 7 S. Bresinsek et al., *Nucl. Fus.* 57 (2017) 116150
 - 8 R. Neu et al., *J. Nucl. Mater.*, article in press, <https://doi.org/10.1016/j.jnucmat.2018.05.066>
 - 9 A. Calvo et al., *Int. J. Refract. Met. Hard Mater.* 73 (2018) 29
 - 10 C. J. Smithells, *Nature* 139 (1937) 490
 - 11 R. Neu et al., *Fus. Eng. Des.* 124 (2017) 450
 - 12 A. Hermann et al., *Nucl. Mater. Energy* 12 (2017) 205
 - 13 D. Maisonnier et al., *Fus. Eng. Des.* 75 (2005) 1173
 - 14 F. Koch and H. Bolt, *Phys. Scripta T128* (2007) 100
 - 15 A. Manhard et al., *Pract. Metallogr.* 52 (2015) 437
 - 16 A. Manhard et al., *Plasma Sources Sci. Technol.* 20 (2011) 015010
 - 17 K. Schmid and U. von Toussaint, *Nucl. Instr. Meth. B* 281 (2012) 64
 - 18 M. Mayer, *SIMNRA User's Guide*, Report IPP 9/113, Max-Planck-Institut für Plasmaphysik, Garching, Germany, 1997
 - 19 T. F. Silva et al., *Nucl. Instr. Meth. B* 371 (2016) 86
 - 20 E. Saloncon et al., *J. Nucl. Mater.* 376 (2008) 160
 - 21 P. Wang et al., *Nucl. Instr. Meth. B* 300 (2013) 54
 - 22 G. Alefeld and J. Völkl (ed.), *Hydrogen in Metals I*, Topics in Applied Physics Vol 28, Springer, Berlin 1978, chapter 12 by J. Völkl and G. Alefeld
 - 23 R. Dus and M. Smialowski, *Acta Metallurgica* 15 (1967) 1611; see also Fisher, D. J. (ed.), *Hydrogen Diffusion in Metals – A 30-Year Retrospective*, Scitec Publications Ltd., Zurich 1999
 - 24 E. Fromm and G. Hörz, *Int. Metals Reviews* 25 (1980) 269
 - 25 K. Schmid et al., *J. Nucl. Mater.* 426 (2012) 247
 - 26 D. Stork et al., *J. Nucl. Mater.* 455 (2014) 277

Paper length

Main text: 3632 words

Figure captions: 395 words

Figures total: 130 + 130+130+ 150+176 +150 + 150 = 1016 words

Total: 3632 + 395 + 1016 = 5043 words. (limit is 5500 words)

Figure captions:

Figure 1: SEM image of HPM 1850 in backscatter electron contrast. The different grey shades are due to grain orientation contrast; the dark area surrounding the tungsten grains is the nickel/iron matrix. The scale bar at the bottom right is 200 μm .

Figure 2: SEM image of W10Cr0.5Y in backscatter electron contrast. The scale bar at the bottom right is 5 μm . The dark areas are a chromium-rich phase, see text.

Figure 3: SEM image of the tungsten reference material in backscatter electron contrast. The different grey shades are due to grain orientation contrast. The scale bar at the bottom right is 5 μm . The image was taken after the experiments

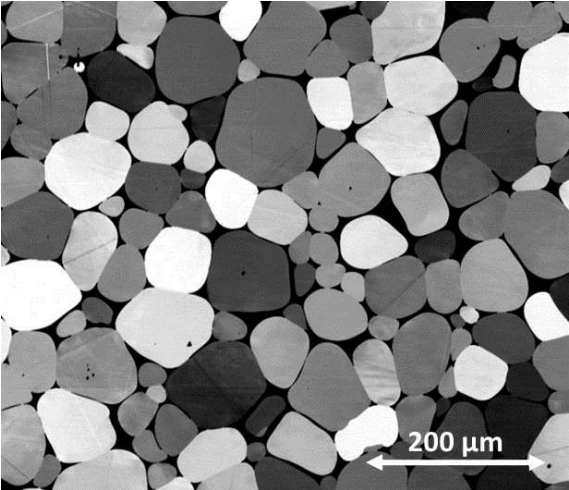
Figure 4: Total released D amounts in the thermal desorption experiment as a function of implantation fluence for HPM 1850 and tungsten reference material. For HPM 1850 there are two data points per fluence: Sample #1 blue crosses, sample #2 red circles. The black squares are the data from the tungsten reference material.

Figure 5: Thermal desorption data for two HPM 1850 samples (solid line/ blue and dashed line/red) and one tungsten reference sample (black solid line with symbols) implanted with the highest deuterium fluence of 10^{25} m^{-2} . The left ordinate axis gives the mass spectrometer mass-4 signal in counts per second. The right ordinate axis shows the furnace temperature. The temperature ramp is shown as a straight line up to 1050°C for the reference tungsten sample. The dashed line indicates the end of the ramp at 850°C for the HPM 1850 samples. The temperature ramp started from room temperature.

Figure 6: Total released D amounts in the thermal desorption experiment as a function of implantation fluence for W10Cr0.5Y and tungsten reference material. Blue crosses and green squares: W10Cr0.5Y; black squares: tungsten reference. For W10Cr0.5Y there are two data points for the highest and lowest implantation fluence and one data point for the intermediate fluence. The tungsten reference data are the same as in figure 3.

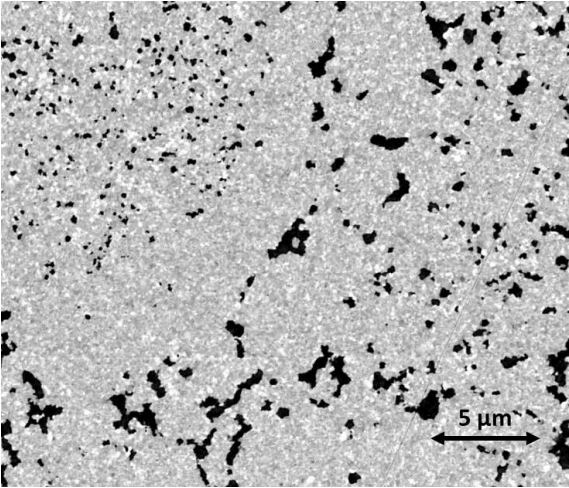
Figure 7: Comparison of the total released D in the thermal desorption (TD) measurements with the integrated depth profile from Nuclear Reaction Analysis (NRA). TD data: blue crosses and green squares for W10Cr0.5Y and black squares for the tungsten reference material. NRA data: blue and green circles for W10Cr0.5Y and black open squares for the tungsten reference material. The TD data are the same as in figure 6.

Figure 1, 7.5 * 6.5 cm



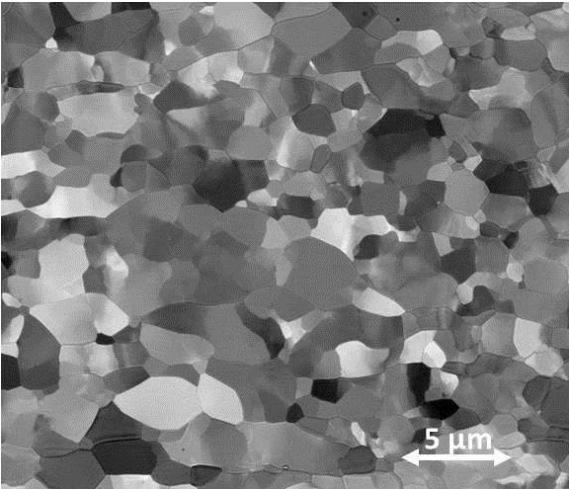
6.5 cm * 20 words/cm = 130 words

Figure 2 7.5 * 6.5 cm



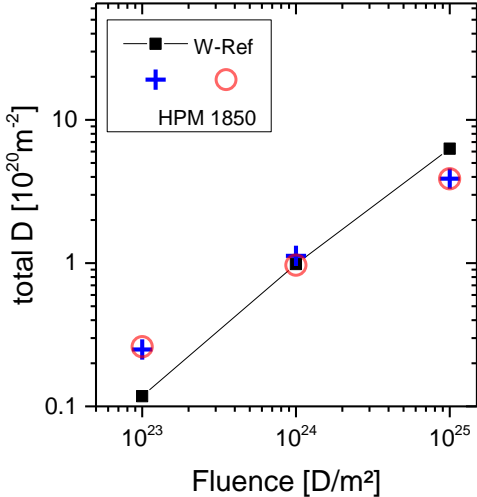
6.5 cm * 20 words/cm = 130 words

Figure 3: 7.5*6.5 cm



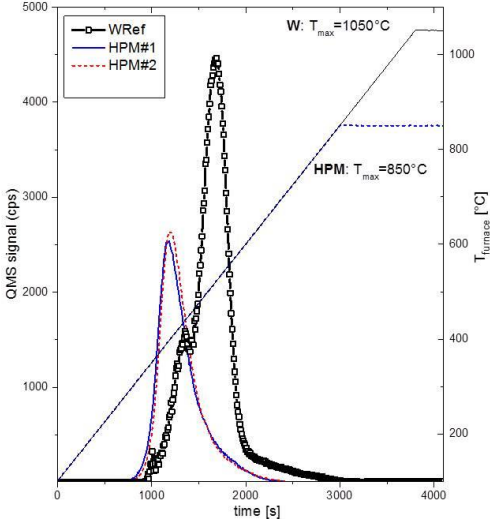
6.5 cm * 20 words/cm = 130 words

Figure 4: 7.5*7.5 cm



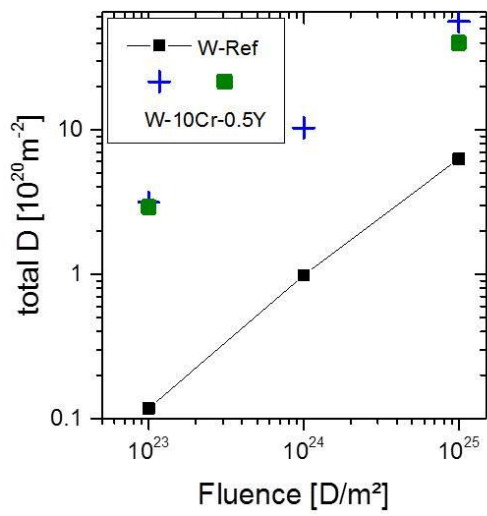
7.5 cm * 20 words/cm = 150 words

Figure 5: 7.5*8.8 cm



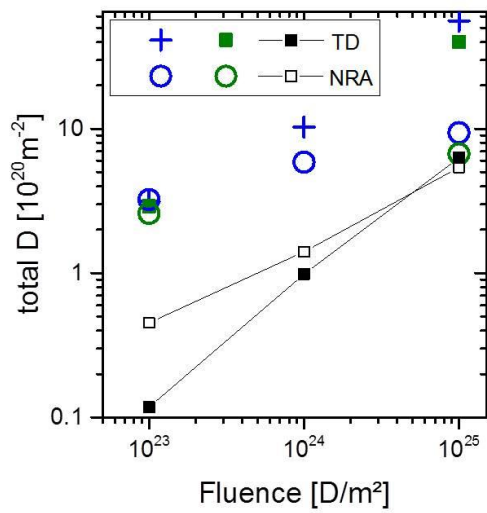
8.8 cm * 20 words/cm = 176 words

Figure 6: 7.5*7.5 cm



7.5cm * 20 words/cm = 150 words

Figure 7: 7.5*7.5 cm



7.5 cm * 20 words/cm = 150 words